

Supplemental Table and Figures

Cholinergic modulation of neuronal excitability and recurrent excitation-inhibition in prefrontal cortex circuits: implications for gamma oscillations

Diego E Pafundo, Takeaki Miyamae, David A Lewis and Guillermo Gonzalez-Burgos

Supplemental Table 1

	Firing PCs (6)	Non Firing PCs (15)	P
Rm M Ω	188.8 \pm 40.3	200.2 \pm 24.2	0.807
τ m (ms)	22.7 \pm 2.4	21.5 \pm 1.3	0.656
AP amplitude (mV)	55.6 \pm 6.1	59.2 \pm 2.8	0.537
AP half width (ms)	1.33 \pm 0.14	1.43 \pm 0.13	0.637
AP threshold (mV)	-42.5 \pm 1.9	-40.7 \pm 2.8	0.381
AP adaptation ratio	5.09 \pm 0.99	4.78 \pm 0.57	0.917
AHP (mV)	-9.3 \pm 1.2	-9.0 \pm 0.9	0.846

Membrane and action potential properties of PCs that fire and PCs that do not fire APs during bath application of CCh. All properties were compared by student's t-test.

Fig S1

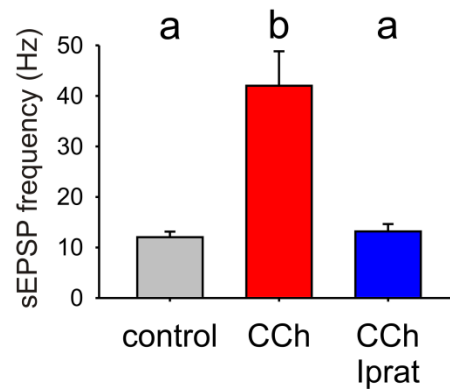


Figure S1.

Muscarinic AChR blockade reverts the increase of the frequency of sEPSPs in FSNs produced by CCh. sEPSP frequency in control conditions and in the presence of 10 μ M CCh or 10 μ M Ipratropium + 10 μ M CCh. Data are means \pm SEM, n=20. Repeated Measures ANOVA indicated significant differences between group means; $F_{2,38}=16.78$, $p<0.001$. Individual groups not sharing the same letter are significantly different, $p<0.05$ post-hoc comparisons with Tukey test.

Fig S2

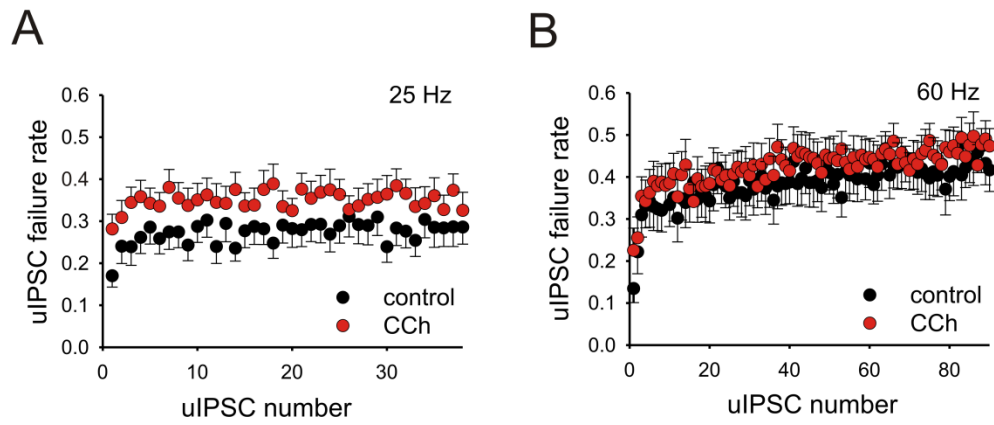


Figure S2.

The effects of CCh on uIPSC failure rate at FSN-PC synapses during gamma frequency activity are consistent with presynaptic modulation. uIPSC failure rate during the trains at 25 (A) and 60 Hz (B) in control and with 10 μ M CCh. Data are mean \pm SEM n=14-15 pairs.

Fig S3

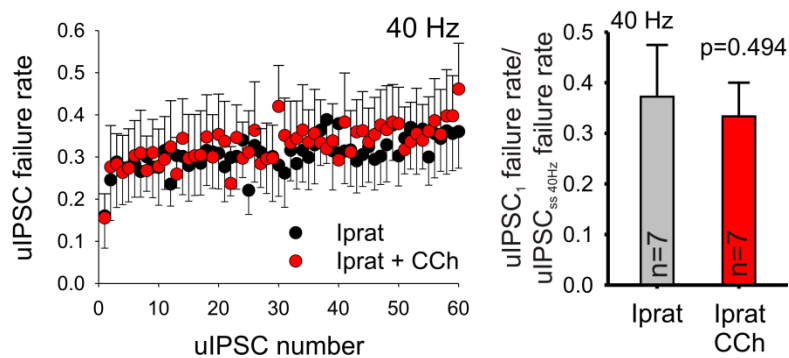


Figure S3.

The effects of CCh on uIPSC the failure rate at FSN-PC synapses can be blocked by a mAChR antagonist. Left: uIPSC failure rate during the trains at 40 Hz in the presence of ipratropium (10 μ M) and with 10 μ M ipratropium + 10 μ M CCh. Data are mean \pm SEM n=7 pairs. Right: A ratio of relative failure rates during the trains (failure rate for uIPSC₁ over the failure rate for the steady state uIPSC) was calculated for experiments in the presence of ipratropium (10 μ M) and with 10 μ M ipratropium + 10 μ M CCh for the 40 Hz trains. Data are shown as mean \pm SEM. p=0.494 (paired t-test).

Fig S4

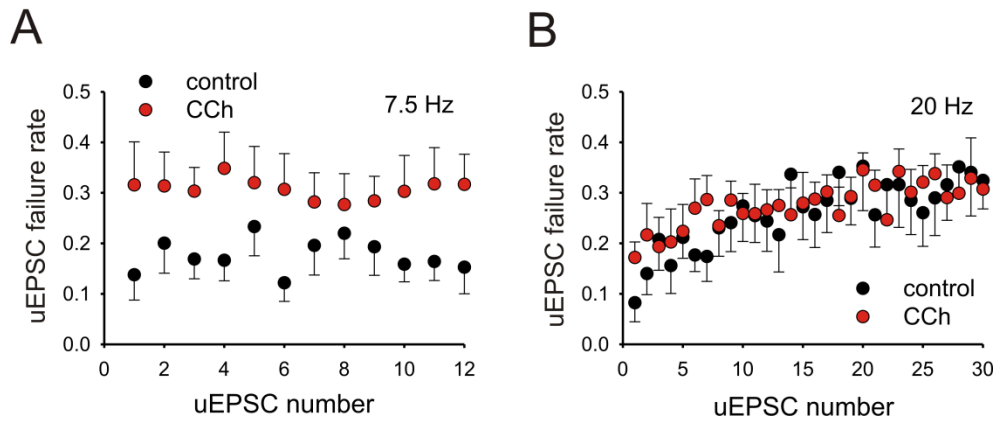


Figure S4.

The effects of CCh on uEPSC failure rate at PC-FSN synapses during gamma frequency activity are consistent with presynaptic modulation. uEPSC failure rate during the trains at 7.5 (A) and 20 Hz (B) in control and with 10 μ M CCh. Data are mean \pm SEM (n=7).

Fig S5

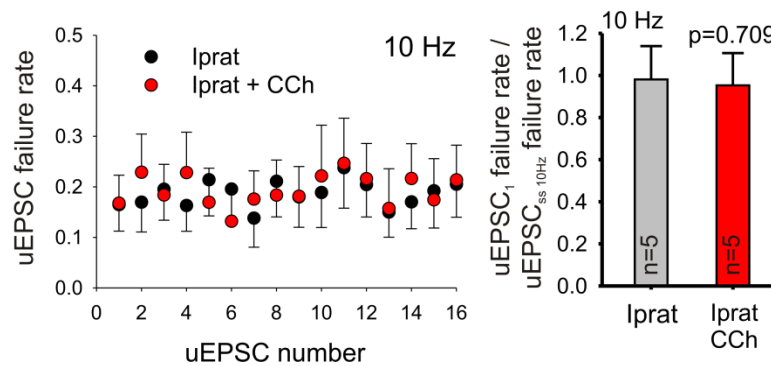


Figure S5.

The effects of CCh on uEPSC failure rate at PC-FSN synapses can be blocked by a mAChR antagonist. Left: uEPSC failure rate during the trains at 10 Hz in the presence of ipratropium (10 μ M) and with 10 μ M ipratropium + 10 μ M CCh. Data are mean \pm SEM n=5 pairs. Right: A ratio of relative failure rates during the trains (failure rate for uEPSC₁ over the failure rate for the steady state uEPSC) was calculated for experiments in the presence of ipratropium (10 μ M) and with 10 μ M ipratropium + 10 μ M CCh for the 10 Hz trains. Data are shown as mean \pm SEM. p=0.709 (paired t-test).

Fig S6

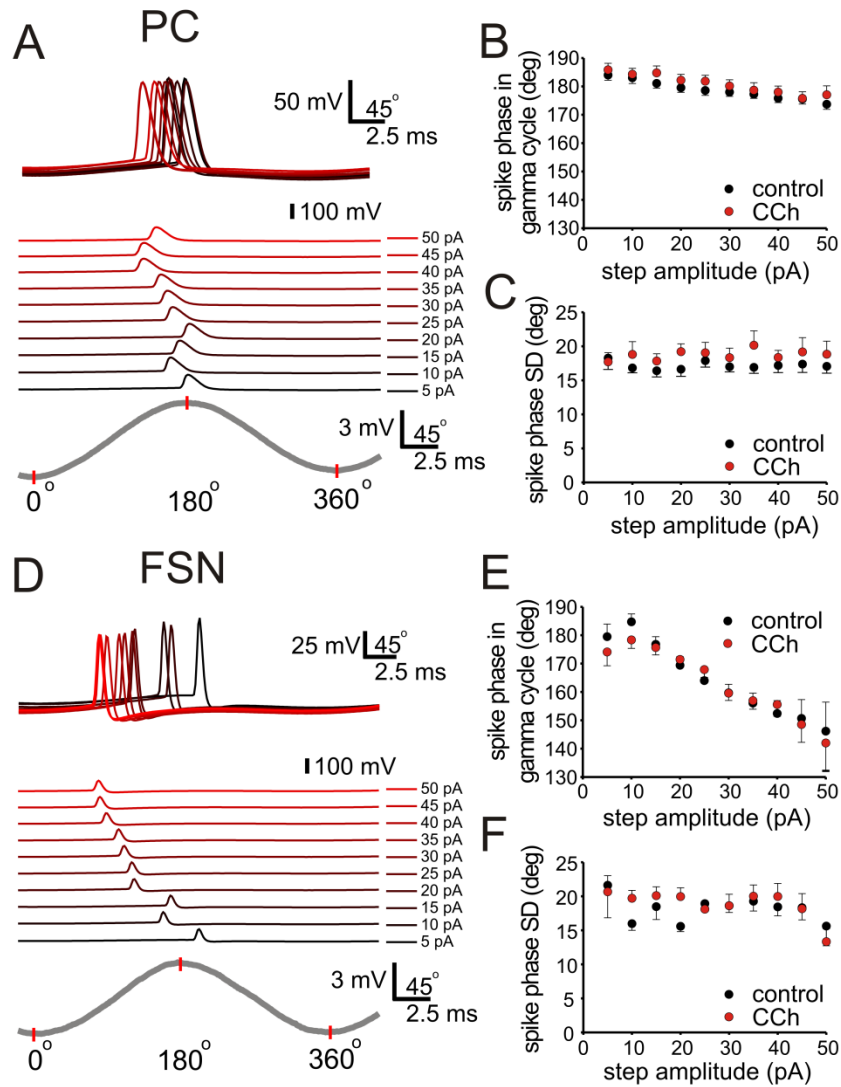


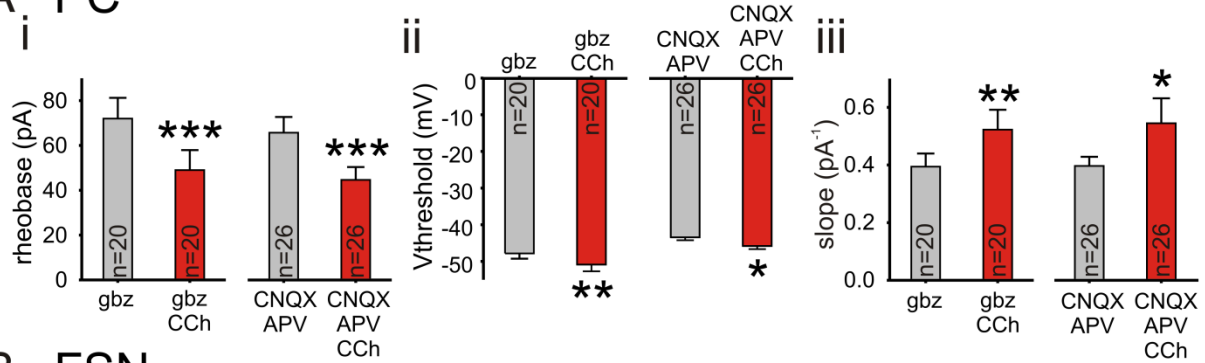
Figure S6.

Modulation of spike timing in PCs and FSNs during the gamma cycle. **A**, Representative traces of the AP firing in a PC during individual cycles of the gamma wave stimulus protocol, as the current step amplitude increased from 5 to 50 pA above rheobase, in 5 pA increments. The APs evoked by each current step amplitude are shown superimposed (top traces) or separately (middle traces). The grey trace at the bottom depicts the change in the PC membrane potential produced by subthreshold gamma

wave stimulation. **B**, Spike phase in PCs as a function of gamma wave current step amplitude in the absence (control) and presence of 10 μ M CCh (CCh). The spike phase was measured from a reference point of 0° placed at the minimum of the subthreshold membrane potential oscillation, as indicated in the lower trace of **A**. Data are mean \pm SEM, $n=21$ RM ANOVA revealed a significant effect of gamma wave current step amplitude of spike phase ($F_{9,174}=3.937$; $p<0.001$) and a small but significant CCh effect on spike phase ($F_{1,174}=5.986$ $p=0.015$). Post-hoc contrasts did not show significant effects of CCh on spike phase at each current amplitude ($P>0.05$). **C**, Standard deviation of the spike phase in PCs as a function of the gamma wave current step amplitude in control conditions and with 10 μ M CCh. Symbols represent mean \pm SEM, $n=21$. RM ANOVA analysis showed that the standard deviation of spike phase was not significantly affected by the current step amplitude ($F_{9,174}=0.202$ $p=0.994$) but was changed by CCh ($F_{1,174}=7.017$ $p=0.008$), although post-hoc tests did not find significant differences between control and CCh at each current step amplitude ($P>0.05$). **D**, Representative traces of the AP firing in a FSN during individual cycles of the gamma wave stimulus protocol, at increasing amplitudes of the current step above the rheobase (from 5 pA shown in black to 50 pA in red). As in **A**, the top panel shows the traces superimposed and the middle panel shows the same traces separately. The gray trace at the bottom shows the change in membrane potential by subthreshold gamma wave stimulus. **E**, **F**, Spike phase (**E**) and its standard deviation (**F**) for APs in FSNs ($n=20$) recorded in control conditions and in the presence of CCh as described for PCs in **B** and **C**. RM ANOVA revealed a significant effect of current step amplitude on FSN spike phase ($F_{9,170}=18.217$ $p<0.001$) and an absence of effect of CCh effect on the FSN spike phase ($F_{1,170}=0.189$ $p=0.664$). The FSN spike phase standard deviation (**F**) did not change significantly with stimulus amplitude ($F_{9,170}=0.984$ $p=0.453$) or in the presence of CCh ($F_{1,170}=0.481$ $p=0.488$).

Fig S7

A PC



B FSN

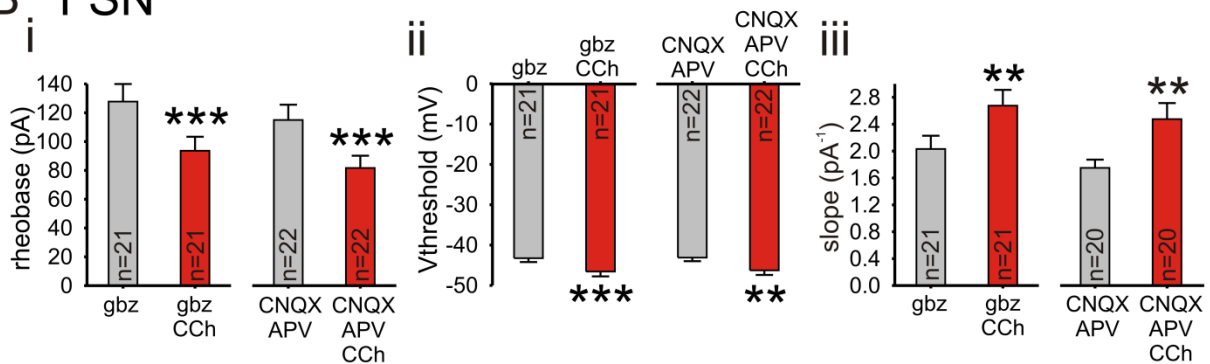


Figure S7.

Effects of gamma wave stimulation in PC (A) and FSNs (B) in the presence of CCh and synaptic receptor blockers. For these experiments, GABA synapses were blocked with the GABA_A receptor antagonist gabazine (gbz, 10 μ M) and glutamate synapses were blocked using the glutamate receptor antagonists CNQX (10 μ M) and APV (50 μ M). Gamma wave stimulation was applied first in the presence of the synaptic blockers and then, after adding 10 μ M CCh in the presence of synaptic blockers. A, The rheobase (i), Vthreshold (ii) and slope of the input-output relation (iii) determined for PCs. B, The rheobase (i), Vthreshold (ii) and slope of the input-output relation (iii) determined for FSNs. Data are mean \pm SEM, n=20-26. * p<0.05, ** p<0.01, *** p<0.001 (paired t-test).